

1 Why care about muons ? ¹

- What is the origin of the patterns of quark and lepton masses and mixings?
- Most models predict new phenomena involving charged leptons which may even be required to solve the puzzle.
- Predicted rates for LFV decays are often within reach experimentally.
- The sensitivity to the muon edm could be raised by factor 5000.
- The experimental sensitivity for $\mu^+ \rightarrow e^+ \gamma$ is limited by accidental $e^+ \gamma$ coincidences and muon beam intensities have to be reduced now already.
- Searches for $\mu - e$ conversion are limited by the available beam intensities and large improvements in sensitivity may still be achieved.
- What about $\mu \rightarrow 3e$ ² (20 year old upper limit 10^{-12}) ?

¹Flavour phenomena in the charged lepton sector have been discussed in a recent series of CERN workshops. Report available.

²Discussed at a PSI workshop two months ago

2 muon EDM

$$\mathcal{H} \sim d\vec{E} \cdot \vec{S}$$

- EDMs violate CP (and we need that) and are predicted by many BSM scenarios.
- Present limits already severely constrain parameter space and large improvements are still expected.
- Atoms can have enormous enhancement factors thanks to their large internal E fields.

Current constraints within three representative classes of EDMs.

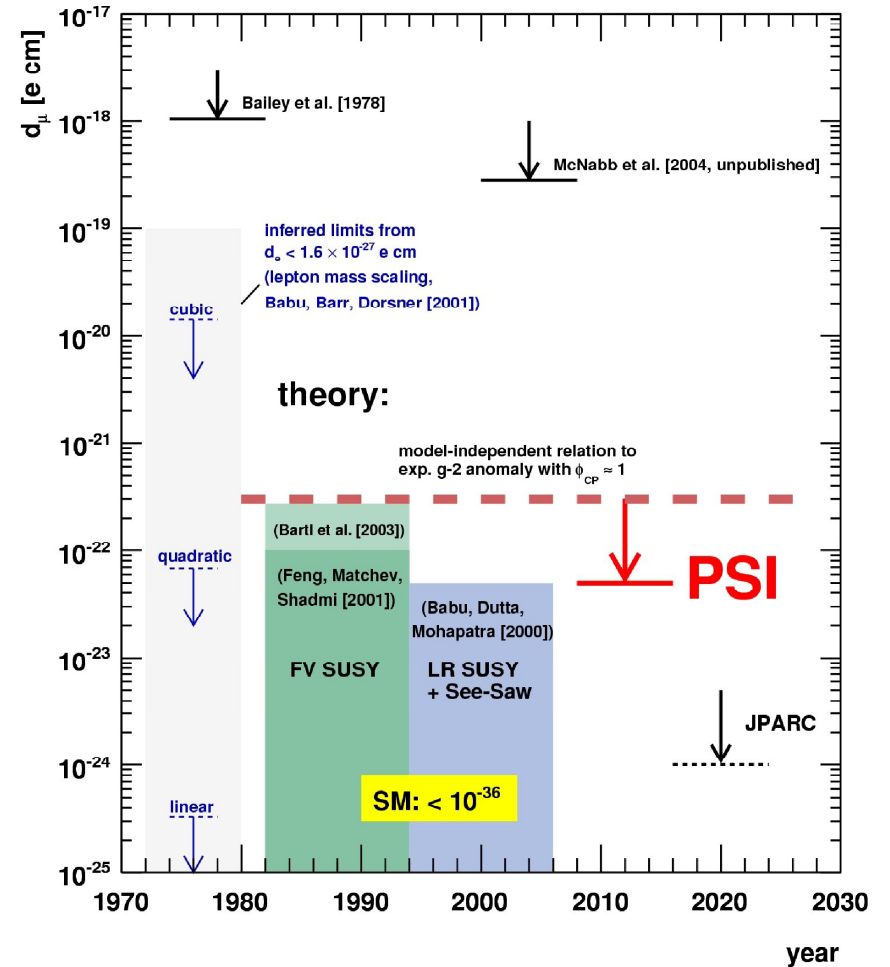
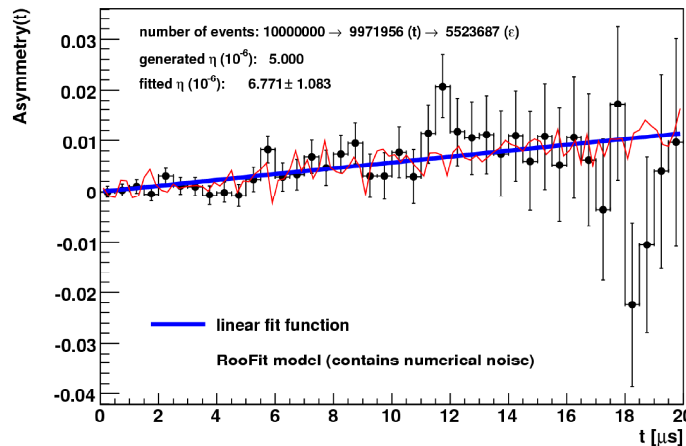
system	fundamental dependence	current bound (e cm)
atom	$d_{\text{para}} \sim 10\alpha^2 Z^3 d_e$	$ d_{\text{Tl}} < 9 \times 10^{-25}$
atom	$d_{\text{dia}} \sim 10Z^2 (R_N/R_A)^2 \tilde{d}_q$	$ d_{\text{Hg}} < 2 \times 10^{-28}$
neutron	$d_n \approx 1.4(6) \times (d_d - 0.25d_u) + 1.1(5) \times e(\tilde{d}_d + 0.5\tilde{d}_u) + 20 \text{ MeV} \times e w$	$ d_n < 3 \times 10^{-26}$

- Muon EDM from g-2 experiment: $d_\mu < 2.4 \times 10^{-19}$ e cm.
- Muon g-2 indirectly gives $d_\mu \lesssim 10^{-22}$ e cm.
- Most models give $d_\mu/d_e \propto m_\mu/m_e$ so $d_\mu < 10^{-25}$ e cm.

Feasibility at PSI studied by Andreas Adelman, Klaus Kirch, Thomas Schietinger, Andreas Streun and Gerco Onderwater (KVI).³

- Inject muons one by one in a storage ring
- Apply radial E field to cancel $g-2$ precession
- Look for build up of vertical muon spin (and so decay) asymmetry

1 minute data taking at present e_μ limit



³<http://amas.web.psi.ch/projects/muonedm/muEDM20070704.pdf>

Programm $\mu \rightarrow 3e$ Workshop (<https://midas.psi.ch/elog/MEEE/>)

Welcome	Stefan Ritt	PSI
<i>purpose of the exercise</i>		
Motivation	Andries van der Schaaf	UZH
<i>$\mu \rightarrow 3e$ v.s. $\mu \rightarrow e\gamma$ v.s. $\mu - e$ conversion</i>		
SINDRUM I	Willi Bertl	PSI
<i>the best result since 20 years</i>		
Design criteria for a new $\mu \rightarrow 3e$ experiment	Andries van der Schaaf	UZH
<i>limitations to the sensitivity</i>		
Ideas for a new $\mu \rightarrow e^+e^+e^-$ experiment	Roland Horisberger	PSI
<i>a large radial TPC with fine-grained readout</i>		
ΠE5 beam line	Peter-Raymond Kettle	PSI
<i>the MEG experience</i>		
Active targets IKAR & MAYA	Oleg Kiselev	PSI
<i>alternatives mainly for heavy fragments</i>		
MuCAP TPC	Malte Hildebrandt	PSI
<i>a TPC based on hydrogen</i>		
Geiger mode APDs	Dieter Renker	PSI
<i>from strips to pads for the plastic scintillator</i>		

3 $\mu \rightarrow 3e$ has many more diagrams than $\mu \rightarrow e\gamma$

Testing Supersymmetry with Lepton Flavor Violating tau and μ decays

Ernesto Arganda and Maria J. Herrero

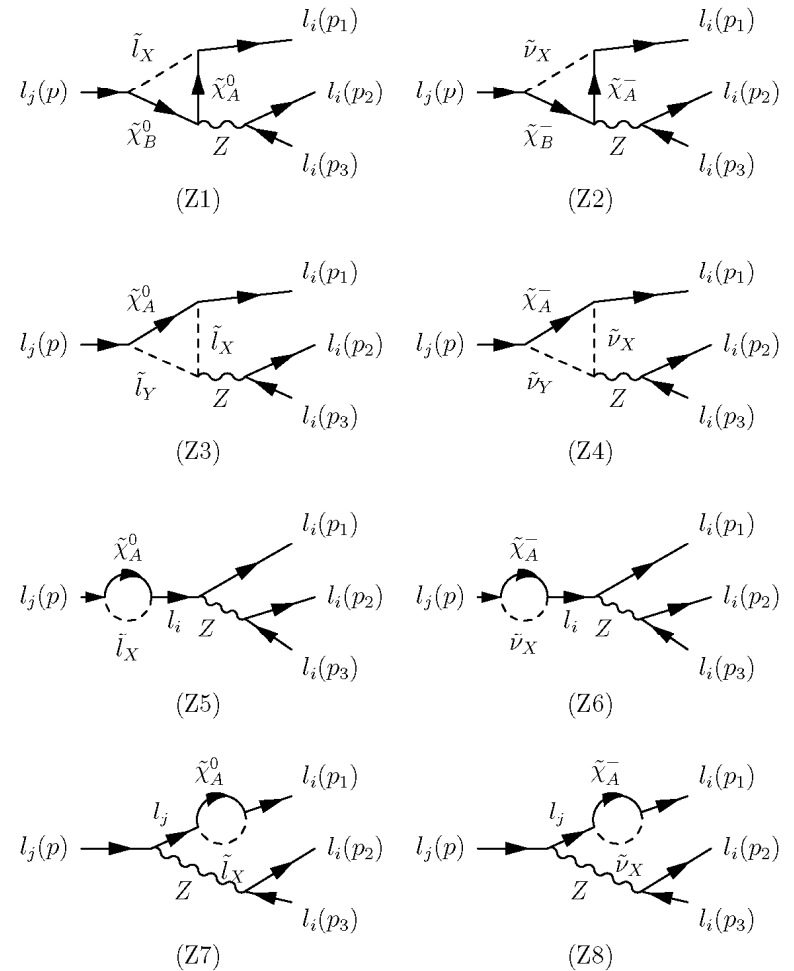
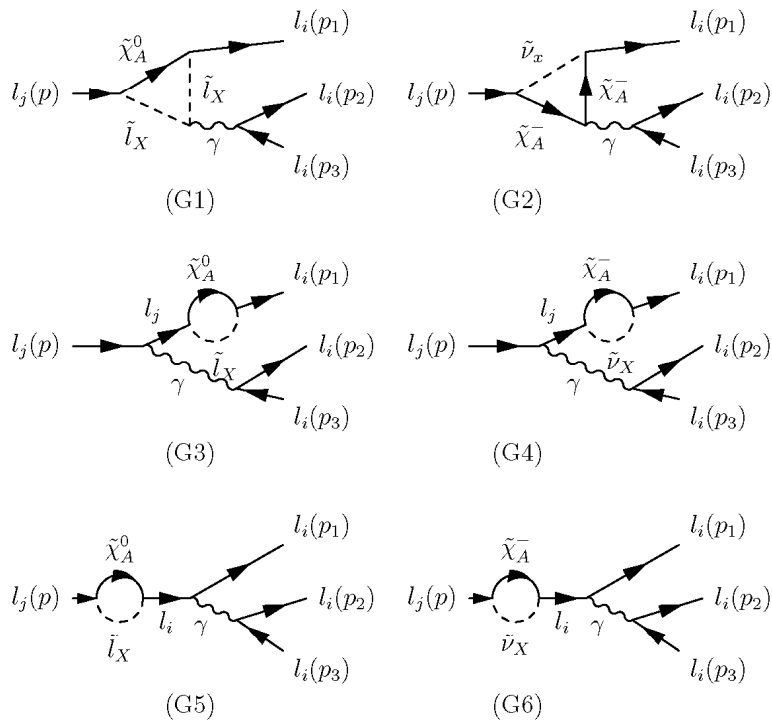


FIG. 1: γ -penguin diagrams contributing to the $l_j^- \rightarrow l_i^- l_i^- l_i^+$ decay

FIG. 2: Z-penguin diagrams contributing to the $l_j^- \rightarrow l_i^- l_i^- l_i^+$ decay

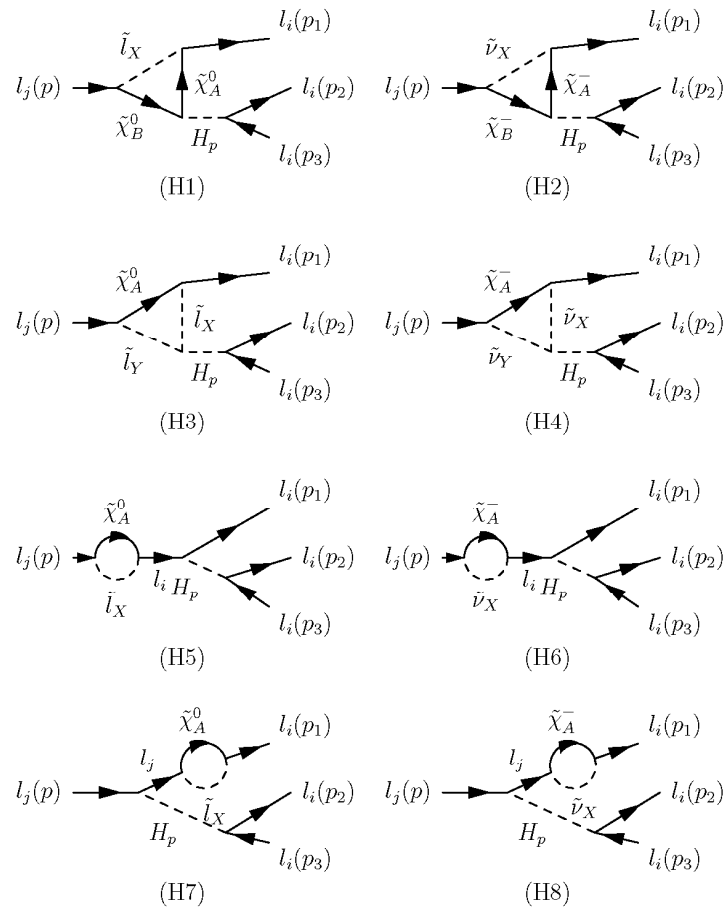


FIG. 4: Higgs-penguin diagrams contributing to the $l_j^- \rightarrow l_i^- l_i^- l_i^+$ decay. Here

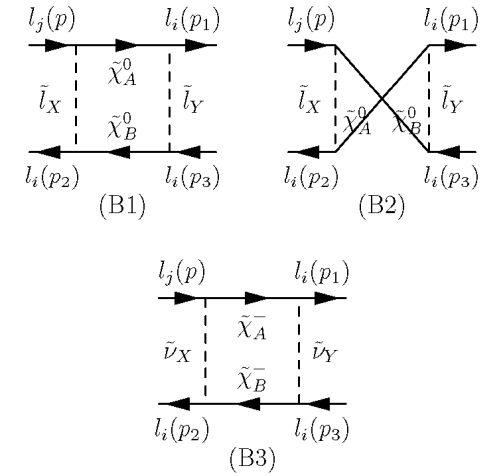
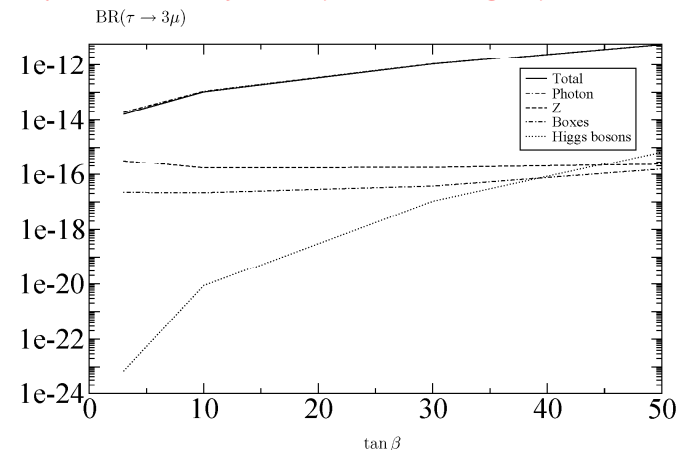


FIG. 3: Box-type diagrams contributing to the $l_j^- \rightarrow l_i^- l_i^- l_i^+$ decay

unfortunately, the photonic graphs dominate



3.1 A recent example: the Littlest Higgs Model

An alternative to SUSY recently developed by Arkani-Hamed et al.

A (The ?) minimal extension of the SM "weakly coupled to new physics" at the TeV scale:

- below 1 TeV nothing changes and around 1 TeV a handful of additional particles are predicted.

Buras et al., 2007

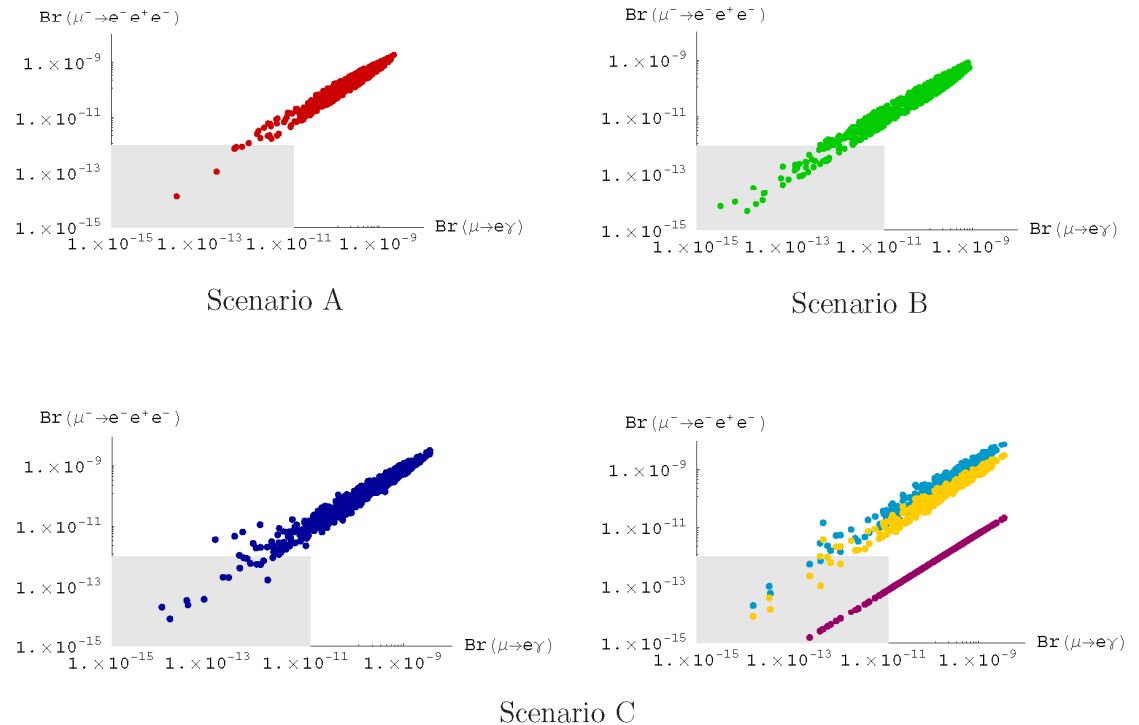


Figure 9: Correlation between $\mu \rightarrow e\gamma$ and $\mu^- \rightarrow e^- e^+ e^-$ in the scenarios of Section 12.2. In the right plot of Scenario C we show the contributions to $\mu^- \rightarrow e^- e^+ e^-$ from $\bar{D}'_{odd}{}^{\mu e}$ (purple, lowermost), $\bar{Z}'_{odd}{}^{\mu e}$ (orange, middle) and $\bar{Y}'_{e,odd}{}^{\mu e}$ (light-blue, uppermost) separately. The shaded area represents the experimental constraints.

decay	$f = 1000 \text{ GeV}$	$f = 500 \text{ GeV}$	exp. upper bound
$\mu \rightarrow e\gamma$	$1.2 \cdot 10^{-11} (1 \cdot 10^{-11})$	$1.2 \cdot 10^{-11} (1 \cdot 10^{-11})$	$1.2 \cdot 10^{-11}$ [17]
$\mu \rightarrow e e^+ e^-$	$1.0 \cdot 10^{-12} (1 \cdot 10^{-12})$	$1.0 \cdot 10^{-12} (1 \cdot 10^{-12})$	$1.0 \cdot 10^{-12}$ [42]
$\mu\text{Ti} \rightarrow e\text{Ti}$	$2 \cdot 10^{-10} (5 \cdot 10^{-12})$	$4 \cdot 10^{-11} (5 \cdot 10^{-12})$	$4.3 \cdot 10^{-12}$ [29]
$\tau \rightarrow e\gamma$	$8 \cdot 10^{-10} (7 \cdot 10^{-10})$	$1 \cdot 10^{-8} (1 \cdot 10^{-8})$	$9.4 \cdot 10^{-8}$ [33]
$\tau \rightarrow \mu\gamma$	$8 \cdot 10^{-10} (8 \cdot 10^{-10})$	$2 \cdot 10^{-8} (1 \cdot 10^{-8})$	$1.6 \cdot 10^{-8}$ [33]
$\tau^- \rightarrow e^- e^+ e^-$	$7 \cdot 10^{-10} (6 \cdot 10^{-10})$	$2 \cdot 10^{-8} (2 \cdot 10^{-8})$	$2.0 \cdot 10^{-7}$ [71]
$\tau^- \rightarrow \mu^- \mu^+ \mu^-$	$7 \cdot 10^{-10} (6 \cdot 10^{-10})$	$3 \cdot 10^{-8} (3 \cdot 10^{-8})$	$1.9 \cdot 10^{-7}$ [71]
$\tau^- \rightarrow e^- \mu^+ \mu^-$	$5 \cdot 10^{-10} (5 \cdot 10^{-10})$	$2 \cdot 10^{-8} (2 \cdot 10^{-8})$	$2.0 \cdot 10^{-7}$ [72]
$\tau^- \rightarrow \mu^- e^+ e^-$	$5 \cdot 10^{-10} (5 \cdot 10^{-10})$	$2 \cdot 10^{-8} (2 \cdot 10^{-8})$	$1.9 \cdot 10^{-7}$ [72]
$\tau^- \rightarrow \mu^- e^+ \mu^-$	$5 \cdot 10^{-14} (3 \cdot 10^{-14})$	$2 \cdot 10^{-14} (2 \cdot 10^{-14})$	$1.3 \cdot 10^{-7}$ [71]
$\tau^- \rightarrow e^- \mu^+ e^-$	$5 \cdot 10^{-14} (3 \cdot 10^{-14})$	$2 \cdot 10^{-14} (2 \cdot 10^{-14})$	$1.1 \cdot 10^{-7}$ [71]
$\tau \rightarrow \mu\pi$	$2 \cdot 10^{-9} (2 \cdot 10^{-9})$	$5.8 \cdot 10^{-8} (5.8 \cdot 10^{-8})$	$5.8 \cdot 10^{-8}$ [33]
$\tau \rightarrow e\pi$	$2 \cdot 10^{-9} (2 \cdot 10^{-9})$	$4.4 \cdot 10^{-8} (4.4 \cdot 10^{-8})$	$4.4 \cdot 10^{-8}$ [33]
$\tau \rightarrow \mu\eta$	$6 \cdot 10^{-10} (6 \cdot 10^{-10})$	$2 \cdot 10^{-8} (2 \cdot 10^{-8})$	$5.1 \cdot 10^{-8}$ [33]
$\tau \rightarrow e\eta$	$6 \cdot 10^{-10} (6 \cdot 10^{-10})$	$2 \cdot 10^{-8} (2 \cdot 10^{-8})$	$4.5 \cdot 10^{-8}$ [33]
$\tau \rightarrow \mu\eta'$	$7 \cdot 10^{-10} (7 \cdot 10^{-10})$	$3 \cdot 10^{-8} (3 \cdot 10^{-8})$	$5.3 \cdot 10^{-8}$ [33]
$\tau \rightarrow e\eta'$	$7 \cdot 10^{-10} (7 \cdot 10^{-10})$	$3 \cdot 10^{-8} (3 \cdot 10^{-8})$	$9.0 \cdot 10^{-8}$ [33]
$K_L \rightarrow \mu e$	$4 \cdot 10^{-13} (2 \cdot 10^{-13})$	$3 \cdot 10^{-14} (3 \cdot 10^{-14})$	$4.7 \cdot 10^{-12}$ [50]
$K_L \rightarrow \pi^0 \mu e$	$4 \cdot 10^{-15} (2 \cdot 10^{-15})$	$5 \cdot 10^{-16} (5 \cdot 10^{-16})$	$6.2 \cdot 10^{-9}$ [73]
$B_d \rightarrow \mu e$	$5 \cdot 10^{-16} (2 \cdot 10^{-16})$	$9 \cdot 10^{-17} (9 \cdot 10^{-17})$	$1.7 \cdot 10^{-7}$ [74]
$B_s \rightarrow \mu e$	$5 \cdot 10^{-15} (2 \cdot 10^{-15})$	$9 \cdot 10^{-16} (9 \cdot 10^{-16})$	$6.1 \cdot 10^{-6}$ [75]
$B_d \rightarrow \tau e$	$3 \cdot 10^{-11} (2 \cdot 10^{-11})$	$2 \cdot 10^{-10} (2 \cdot 10^{-10})$	$1.1 \cdot 10^{-4}$ [76]
$B_s \rightarrow \tau e$	$2 \cdot 10^{-10} (2 \cdot 10^{-10})$	$2 \cdot 10^{-9} (2 \cdot 10^{-9})$	—
$B_d \rightarrow \tau \mu$	$3 \cdot 10^{-11} (3 \cdot 10^{-11})$	$3 \cdot 10^{-10} (3 \cdot 10^{-10})$	$3.8 \cdot 10^{-5}$ [76]
$B_s \rightarrow \tau \mu$	$2 \cdot 10^{-10} (2 \cdot 10^{-10})$	$3 \cdot 10^{-9} (3 \cdot 10^{-9})$	—

Table 2: Upper bounds on LFV decay branching ratios in the LHT model, for two different values of the scale f , after imposing the constraints on $\mu \rightarrow e\gamma$ and $\mu^- \rightarrow e^- e^+ e^-$. The numbers given in brackets are obtained after imposing the additional constraint $R(\mu\text{Ti} \rightarrow e\text{Ti}) < 5 \cdot 10^{-12}$. For $f = 500 \text{ GeV}$, also the bounds on $\tau \rightarrow \mu\pi, e\pi$ have been included. The current experimental upper bounds are also given.

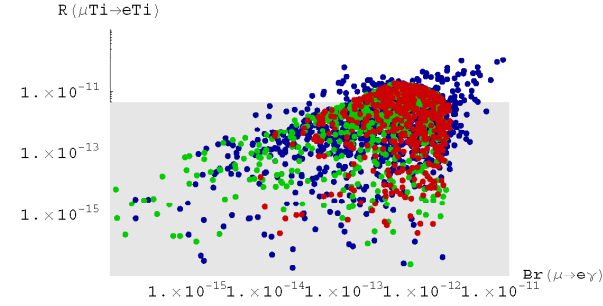


Figure 10: $\mu - e$ conversion rate in ${}^{48}_{22}\text{Ti}$ as a function of $Br(\mu \rightarrow e\gamma)$, after imposing the existing constraints on $\mu \rightarrow e\gamma$ and $\mu^- \rightarrow e^- e^+ e^-$. The shaded area represents the current experimental upper bound on $R(\mu\text{Ti} \rightarrow e\text{Ti})$.

ratio	LHT	MSSM (dipole)	MSSM (Higgs)
$\frac{Br(\mu^- \rightarrow e^- e^+ e^-)}{Br(\mu \rightarrow e\gamma)}$	0.4...2.5	$\sim 6 \cdot 10^{-3}$	$\sim 6 \cdot 10^{-3}$
$\frac{Br(\tau^- \rightarrow e^- e^+ e^-)}{Br(\tau \rightarrow e\gamma)}$	0.4...2.3	$\sim 1 \cdot 10^{-2}$	$\sim 1 \cdot 10^{-2}$
$\frac{Br(\tau^- \rightarrow \mu^- \mu^+ \mu^-)}{Br(\tau \rightarrow \mu\gamma)}$	0.4...2.3	$\sim 2 \cdot 10^{-3}$	0.06...0.1
$\frac{Br(\tau^- \rightarrow e^- \mu^+ \mu^-)}{Br(\tau \rightarrow e\gamma)}$	0.3...1.6	$\sim 2 \cdot 10^{-3}$	0.02...0.04
$\frac{Br(\tau^- \rightarrow \mu^- e^+ e^-)}{Br(\tau \rightarrow \mu\gamma)}$	0.3...1.6	$\sim 1 \cdot 10^{-2}$	$\sim 1 \cdot 10^{-2}$
$\frac{Br(\tau^- \rightarrow e^- e^+ e^-)}{Br(\tau^- \rightarrow e^- \mu^+ \mu^-)}$	1.3...1.7	~ 5	0.3...0.5
$\frac{Br(\tau^- \rightarrow \mu^- \mu^+ \mu^-)}{Br(\tau^- \rightarrow \mu^- e^+ e^-)}$	1.2...1.6	~ 0.2	5...10
$\frac{R(\mu\text{Ti} \rightarrow e\text{Ti})}{Br(\mu \rightarrow e\gamma)}$	$10^{-2} \dots 10^2$	$\sim 5 \cdot 10^{-3}$	0.08...0.15

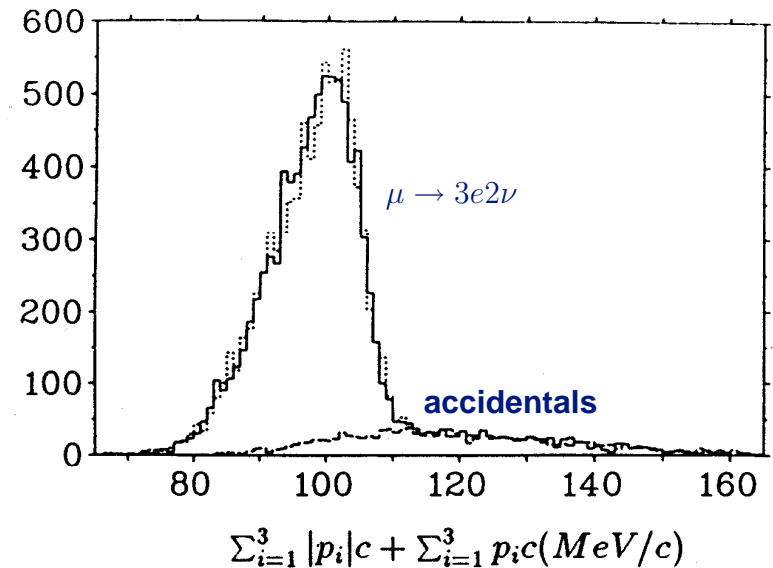
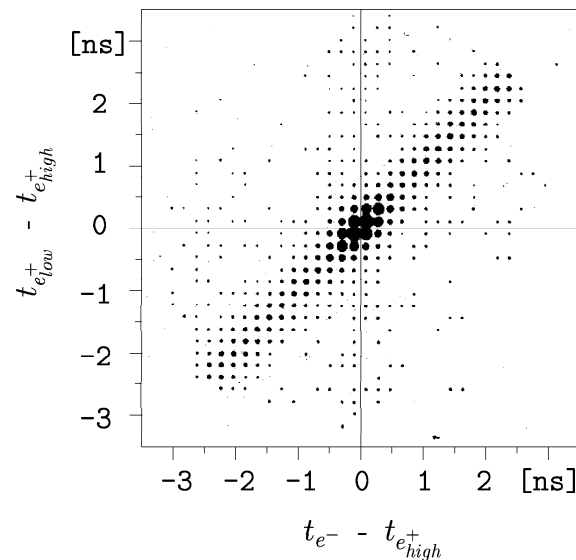
Table 3: Comparison of various ratios of branching ratios in the LHT model and in the MSSM without and with significant Higgs contributions.

4 signature $\mu \rightarrow 3e$ at rest

- total energy, total momentum, (\rightarrow coplanarity).
- Phase space distribution gives additional information if observed.
- In a constant B field the acceptance is defined by the p_t threshold.

5 background

SINDRUM I

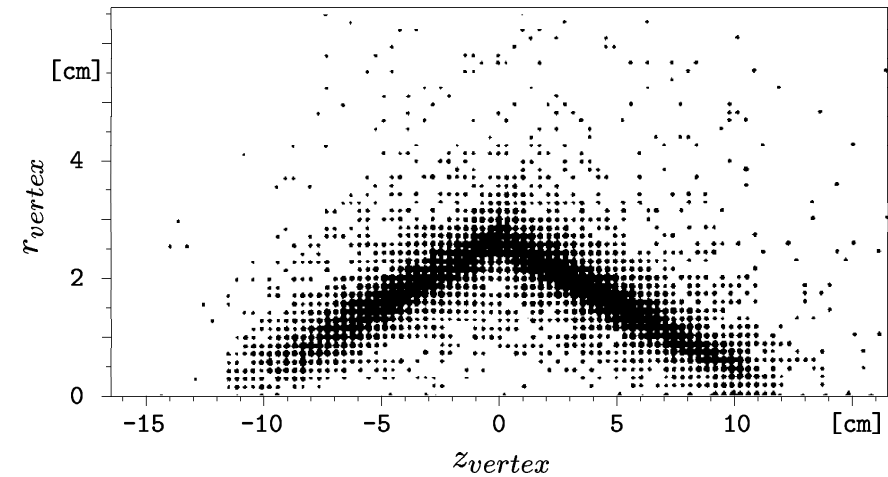


Accidental background

involves low invariant mass e^+e^- pairs produced by photons or by Bhabha scattering.

Suppressing accidental background:

- The three trajectories meet in a common vertex.
- The common vertex has to be in a muon-stop region. For this reason SINDRUM I used a relatively large surface target.
- An active target could lead to a dramatic suppression since one would know the interaction point of γ conversions and Bhabha scatterings. ⁴



⁴Peter Kammel is gratefully acknowledged to bring this up

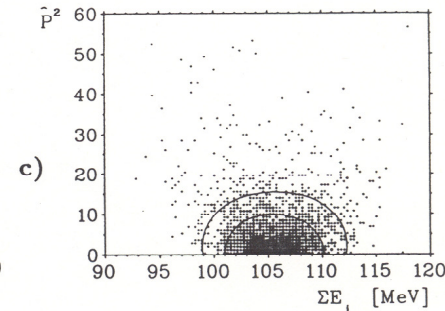
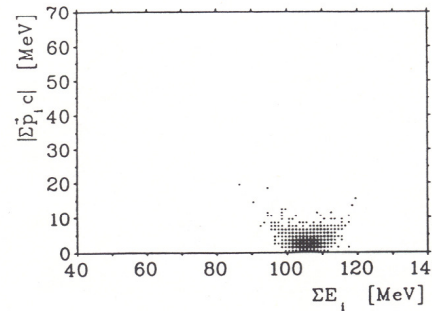
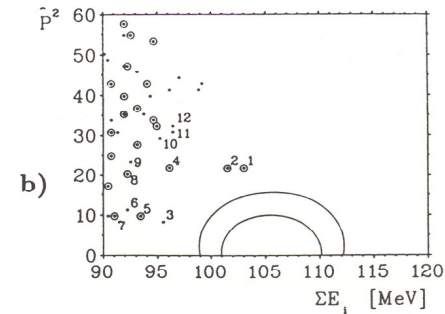
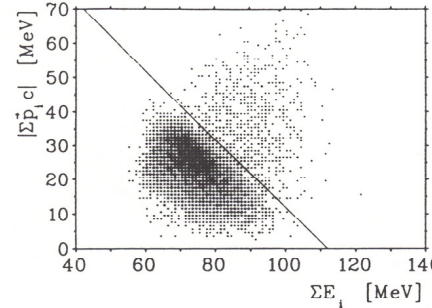
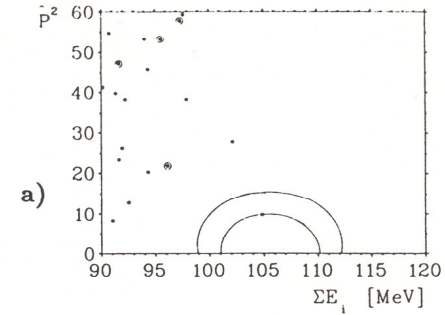
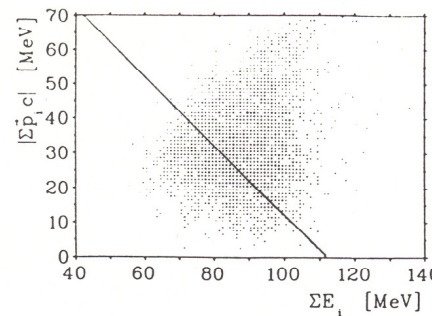
5.1 How to reach a single-event sensitivity of $O(10^{-16})$?

- Measure 100 instead of 10 weeks.
- Raise stop rate from 5×10^6 to $10^9/s$.
- Lower threshold on p_t to gain in acceptance.

χ^2 is a test of the $e^+e^+e^-$ correlation based on time and vertex variables

$$\hat{P}^2 \equiv \left(\frac{P_{\parallel}}{\sigma_{P_{\parallel}}} \right)^2 + \left(\frac{P_{\perp}}{\sigma_{P_{\perp}}} \right)^2$$

\parallel and \perp are defined w.r.t. the decay plane.



5.2 What about background ?

reducing accidental background by improving detector resolutions

assumption ^a	gain factor	background
SINDRUM I	1	40000
$\Delta t \times 0.25$	4	10000
vertex $\times 0.5$	4	2500
energy $\times 0.5$	2	1250
momentum $\times 0.5$	4	300
target size $\times 2$	2	150
target mass/area $\times 0.5$	2	75

^afor example by linear scaling the detector by factor 2

So one would need an additional factor 100.

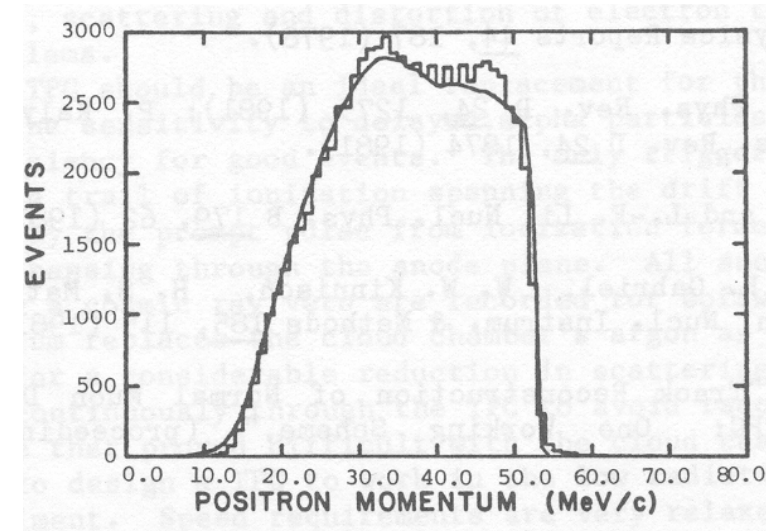
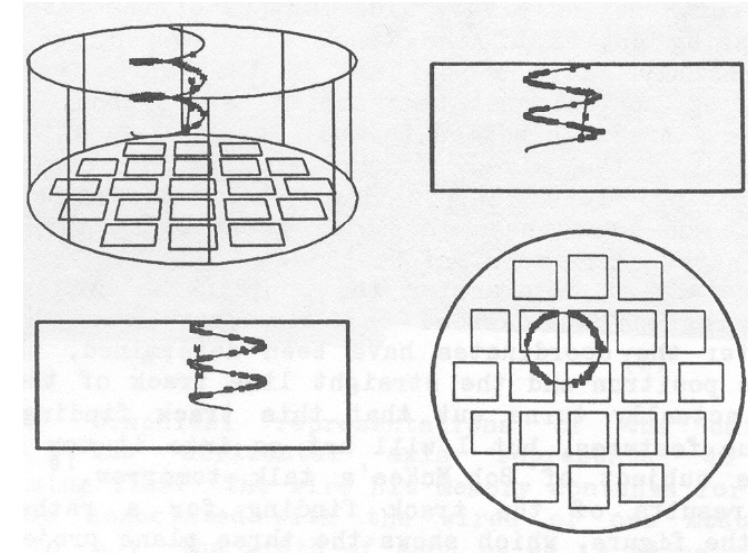
A vertex detector would do the job if it would stand the rate.

5.3 1985: LAMPF TPC

The Time Projection Chamber

AIP Conference Proceedings 108, ed. J.A. Macdonald
contributions by W.W. Kinnison and R.J. McKee

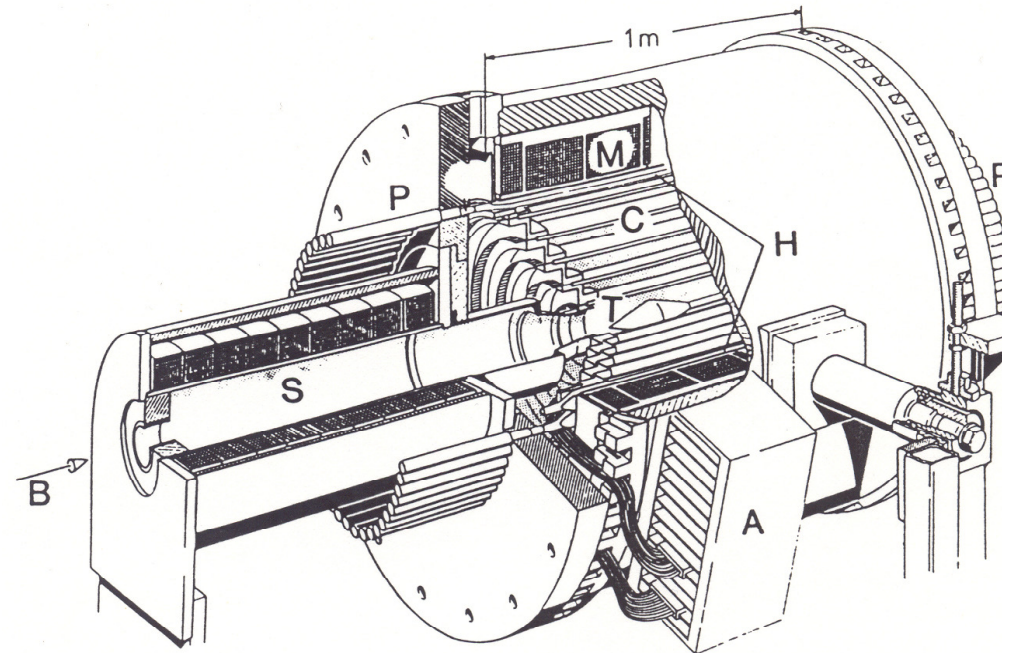
- six authors!
- diameter 122 cm, length 55 cm
- Both the incoming surface muon and its decay positron are observed.
- momentum resolution 1%



5.4 Detector issues

SINDRUM I

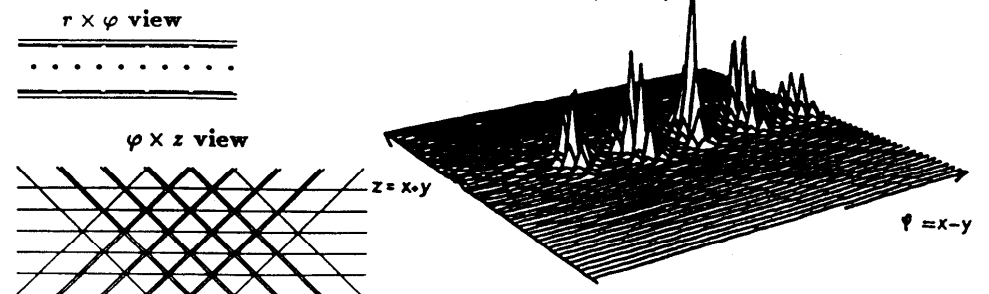
- B beam*
- S focussing solenoid*
- T hollow target*
- C MWPC tracking*
- H plastic hodoscope*



Events triggered with an ultra-thin scintillator.

- Cathodes image the avalanches at the anodes.*
- Phi resolution given by number of anode wires.*
- z resolution 0.2 mm.*

MWPC structure (total mass 30 mg/cm²)



Could one stand the rate?

- extra tracks, combinatorial background

SINDRUM I saw about 0.1 extra track per event at the 50 - 70 ns gating time. If the detector would twice faster there would be 10 random tracks. No problem with sufficient granularity (at least 500 anode wires and cathode strips per plane).

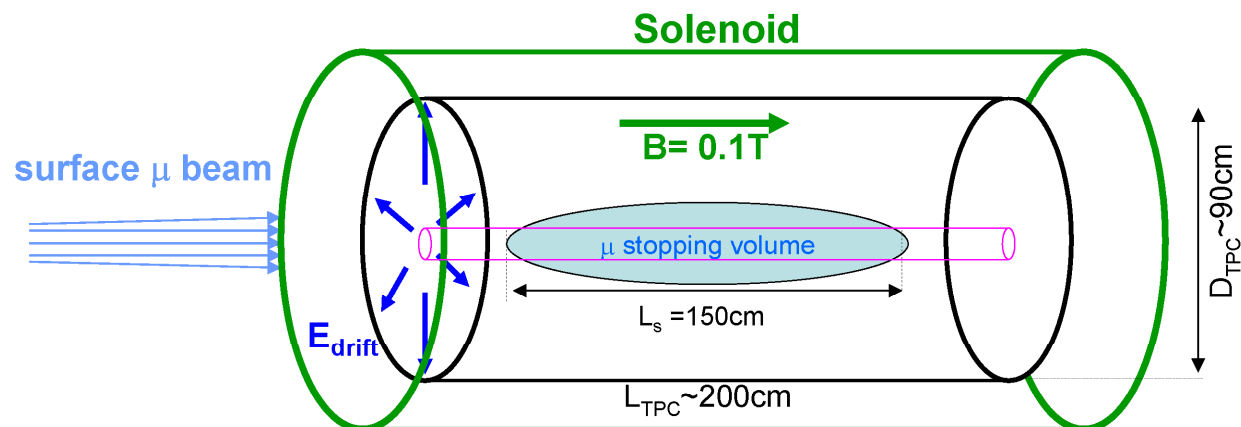
SINDRUM I v.s. MEGA

	SINDRUM I	MEGA	
self-supporting	yes	no	
thickness	10^{-3}	0.3×10^{-3}	rad. length
wire spacing	2	1.3	mm
gas	Ar-C ₂ H ₆ (50-50)	CF ₄ -C ₄ H ₁₀ (80-20)	
gate width	60	30	ns
turns/helix	≈ 1	≈ 5	
peak stop rate	5×10^6	2.5×10^8	1/s
rate per anode	10^5	10^7	1/s
max. fluence	3×10^2	4×10^4	1/mm ² .s

Conclusion: it could work

6 A radial TPC ?

(Roland Horisberger)

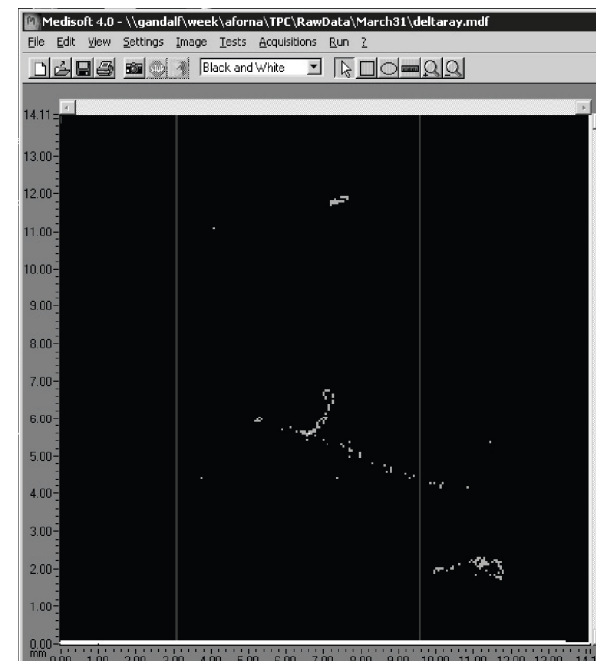


Micro-pattern readout schemes as studied by LCTPC and CERN RD51 (5 years starting now, (Geneva is in) would:

- match the intrinsic precision offered by TPC's,
- stand high particle fluxes by suppression of ion back-flow,
- allow curved structures for radial drift field.

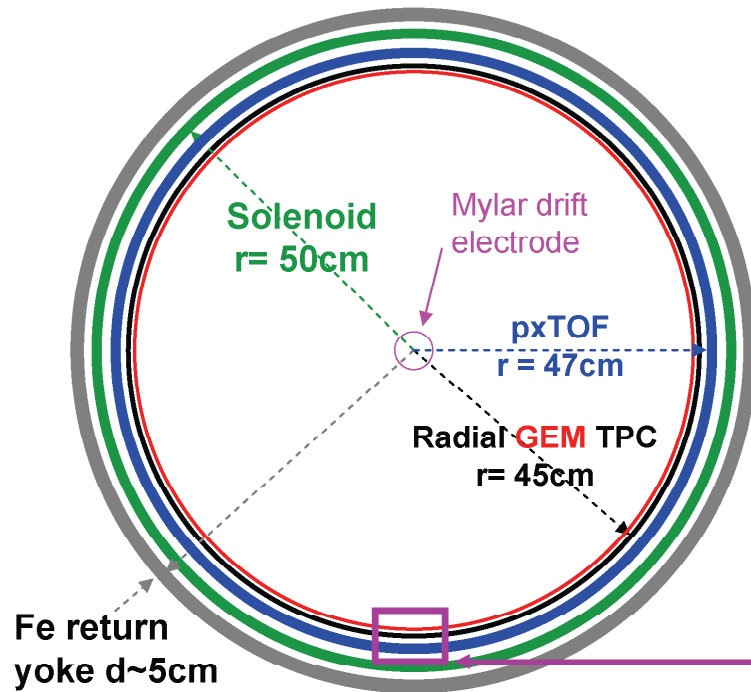
delta electron imaged by LCTPC prototype

$14 \times 14\text{ mm}^2$



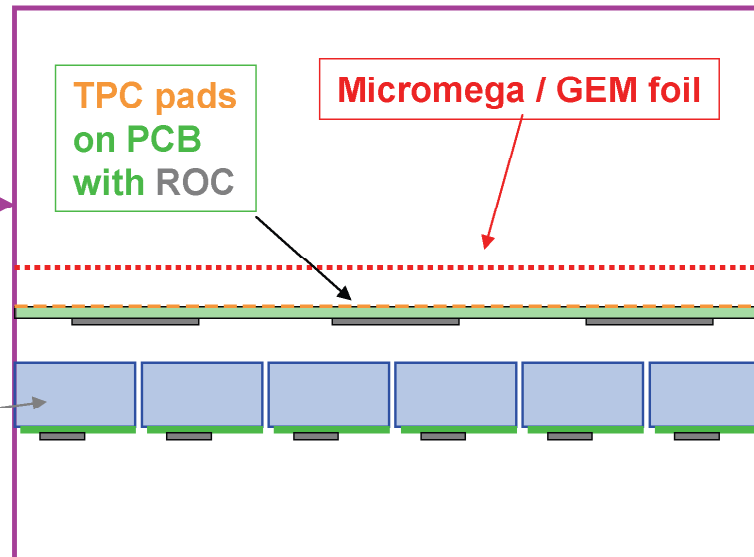


Cross-section of $\mu \rightarrow 3e$ Experiment



Inner surface of solenoid ($\sim 6\text{m}^2$) is equipped:

- 1) GEM or Micromega TPC Pad readout**
0.75mm x 0,75mm pad size, gain $\sim 3\text{-}4\text{K}$
resolution $\sim 200\mu$ in x,y & t (ILC exp.)
few mm double track resolution
- 2) Scint. Pixel TOF system**
1cm x 1cm time resolution $\sim 50\text{psec}$



Scintillator based pixel TOF with Si-PM & TDC ROC

6.1 Open issues

- What is the highest beam intensity that PSI can deliver in 5 years?
Proton current 2→3 mA, optimized target geometry.
- How harmful is loss of central region? One would like to see the $e^+e^+e^-$ vertex.
- A TPC is a slow device. Can events with 10^4 additional muon tracks and decay positrons be analyzed?
- Can triggering be solved? Would a second plastic layer help to trigger fast on charge?
- Would a hybrid scheme (much smaller and faster gated TPC for vertex only combined with 25 ns tracker) solve some of the above?
- Budget? Comparable to MEG?
- Sufficient interest to form an international collaboration?
- Interested colleagues should sign Stefan Ritt's ELOG:
<https://midas.psi.ch/elogs/MEEE/>
- And/Or contact to Klaus Kirch!